Vacuum 125 (2016) 170–179

Contents lists available at ScienceDirect

Vacuum

journal homepage: www.elsevier.com/locate/vacuum

Physico-chemical modification induced in PLGA/OMMT nanocomposite films by Li^{3+} ion beam

Manpreet Kaur [a, *], Surinder Singh [a], Rajeev Mehta [b]

[a] Department of Physics, Guru Nanak Dev University, Amritsar 143005, India
[b] Department of Chemical Engineering, Thapar University, Patiala 147004, India

ARTICLE INFO

Article history:
Received 3 June 2015
Received in revised form
24 December 2015
Accepted 28 December 2015
Available online 31 December 2015

Keywords:
PLGA
Cloisite® 30B
Irradiation effects
Spectroscopy
Fourier transfer infrared (FTIR)
X-ray diffraction (XRD)
Field emission scanning electron microscopy (FESEM)
Optical properties

ABSTRACT

The swift heavy ions irradiation (SHI) effects on the optical, structural and morphological properties of poly(lactide-co-glycolide) (PLGA) nanocomposites containing organically modified nanoclay organo-montmorillonite (OMMT) (Cloisite®30B) has been studied over a range of fluences. Optical analysis of the polymer nanocomposites shows that both the cross-linking phenomenon is caused by swift heavy ion irradiation. The absence of peak of nanoclay in all irradiated nanocomposite samples in Fourier transfer Infrared (FTIR) spectrum demonstrates the formation of complete and/or partial exfoliation. The broadening of peak width of X-ray diffraction (XRD) spectra of irradiated nanocomposite implies an increase in the amorphous phase at higher fluences. Field emission scanning electron microscopy (FESEM) shows the formation of porous structure after irradiation. Presence of nanoclay is found to affect the properties of this degradable copolymer when subjected to ionizing radiation.

© 2015 Elsevier Ltd. All rights reserved.

1. Introduction

Nanocomposite technology consisting of polymer and layered silicates has rapidly grown in the last decade. This combination exhibits remarkably improved thermal, mechanical and various other properties when compared to pure polymer or conventional composites [1]. Nanocomposites are made up of polymer and nano filler where polymer is the continuous phase and the nano filler is the dispersed phase. Usually the nanoclay that is embedded into the host matrix phase is employed to improve the desired properties of the polymer such as mechanical, thermal, barrier and fire retardancy [2]. In PLGA nanocomposites, nanoscale dispersion of OMMT uniformly within the PLGA matrix leads to tremendous interfacial contacts between the matrix and OMMT, which leads to exciting and promising properties than those of bulk polymer phase. The improvement in their properties depends strongly on the adhesion between PLGA and OMMT and the aspect ratio of the OMMT [3–6]. Presence of nanoclay is found to enhance the properties of this degradable copolymer by altering the rate of degradation even at high irradiation fluence.

Since dispersion of clay at nano scale is essential to achieve the improved properties, the processing challenge is to disperse micron size clay particles into millions of platelets in the polymer matrix. The ultrasonic technique is an effective and convenient method in which ultrasonic waves are used to control the nano scale dispersion of clay in polymer matrix [7,8]. The preparation of polymer nanocomposite by incorporation of small amount of organically modified clay (Cloisite® 30B) in PLGA has been reported by Alexander and Dubois [9]. PLGA/clay nanocomposite exhibits remarkably improved moduli, increased strength and heat resistance [10], thermal stability, solvent resistance, hydrophobic character and improvement in other mechanical properties [11] when compared to pure polymer. Another important feature of polymer/layered silicate nanocomposite is that it retards the rate of degradation due to an improvement in the barrier properties by creating a maze or 'tortuous path' that retards the progress of the gas molecules

* Corresponding author.
E-mail address: manpreet984@gmail.com (M. Kaur).

http://dx.doi.org/10.1016/j.vacuum.2015.12.018
0042-207X/© 2015 Elsevier Ltd. All rights reserved.

through the matrix [12].

The irradiation of polymers by SHI beam is a versatile, promising and interesting technique to process and modify the properties of polymers such as structural [13,14] chemical [15], mechanical [16], optical [17,18], thermal [19] and surface morphology [20]. The physical and chemical changes in different polymers which are generally believed to occur are crosslinking, chain scission and structural changes after irradiation with adequate linear energy transfer (LET) of SHI [21–23]. Due to sufficient LET of SHI, more modifications are induced as compared to changes induced by electron or gamma beam. Irradiation creates free radicals which recombine forming the cross-links. The degree of cross-linking depends upon the nature and type of material and irradiation fluence. In the chain scission process, the polymer chains are broken and molar mass decreases [24]. These two phenomena occur at the same time and one may dominate over the other, depending upon the polymer, type of radiation used and fluence. One of the benefits of using SHI is that the relative degree of crosslinking and chain scissioning can be easily controlled by the amount of radiation fluence. The energy of SHI-irradiated beam could also cause the chain scission through breaking of chemical bonds which decreases the band gap energy of polymer and increases the rate of degradation or alternately cause some cross-linking within polymer chains and lower the rate of degradation. When PLGA nanocomposites are irradiated with ion beam at high fluence, chain scission dominates over cross-linking resulting in polymer chains becoming shorter and thus facilitating crystallization. This is so because during chain scission, the molecules become shorter, chains become less entangled and reorientation of molecules can occur which increases the degree of crystallization. As a result of this, film samples become more brittle. Since the clay is ceramic and it is known from many studies in the literature that increase in clay content in polymer matrix leads to increase in brittleness. In the present study, this process happened in all irradiated samples but not in pristine samples. This is not good for some of the typical medical applications of PLGA, because the service life of a PLGA nanocomposites product, which has been subjected to ionizing radiation for sterilization, would be adversely affected. Literature has shown that irradiated and non-irritated PLGA and PLGA nanocomposites have numerous applications in medical and engineering fields [25–29]. Products made from PLGA are widely used inside the human body e.g. absorbable sutures, wound healing materials, artificial skin grafts, orthopedic and resorbable fixation devices, surgical sealant films. These parts have to be sterilized, mostly by radiation, before their use in the human bodies. In addition to desirable properties like swelling behavior, capacity to undergo hydrolysis, biodegradation rate of the polymer, moduli, thermal stability, solvent resistance, PLGA also have low mechanical properties. Upon irradiation, the low mechanical properties go to even lower values. Addition of nano fillers like nano clay tends to increase the mechanical properties quite significantly. Thus, the rationale is to study nano clay reinforced PLGA and its extent of degradation upon irradiation.

The present study is concerned with the radiation effects on PLGA/OMMT (Cloisite® 30B) by SHI. PLGA has several biomedical applications and in general, it is required to be irradiated for sterilization. We have already reported the effect of radiation on PLGA [30]. It is well known from literature that properly dispersed nanoclay in polymer matrix significantly changes the physico-chemical properties as compared to neat PLGA. Therefore in the present study, the effect of nanoclay addition to the morphology (FESEM), chemical bonding (FTIR), optical study (UV–visible) and degree of nanoclay dispersion (XRD) before and after irradiation has been investigated.

2. Experimental

2.1. Materials

PLGA ($M_W = 70{,}000$, as measured by viscometry), consisting of 50/50 poly(lactic acid) and poly(glycolic acid), was purchased from Lakeshore Biomaterials, USA. It was used to prepare nanocomposites by incorporating commercial organically modified clay (Cloisite® 30B) manufactured by Southern Clay, USA, in dichloromethane (DCM) solvent.

2.2. Preparation of nanocomposites

Three different ratios i.e. 1% (wt), 3% (wt) and 5% (wt) of organically modified nanoclay and PLGA were dissolved into DCM solvent separately into 1:12 ratio. The highest clay content was capped at 5% (wt) because it is known from literature that on polymer-clay nanocomposites at a concentration more than 5% (wt), it is very unlikely to prevent clay aggregation [31–33]. To achieve nano-scale dispersion of nanoclay into polymer matrix, ultrasonication probe was used (Ultrasonic processor LABSONIC® Sartorius) for 30 min at a voltage of 115 V, power of 100 W and frequency of 60 Hz. The dispersion was cast on a glass sheet, to obtain films of rectangular shape. These were dried for 48 h at room temperature and further in an oven at 40 °C for a week to give PLGA films of 30 μm thickness.

2.3. Swift heavy ion irradiation

PLGA nanocomposites were irradiated using 50 MeV (Li^{3+}) ion beam under vacuum (10-6 Torr), directed normal to sample surface and at a current of 0.5–1.0 pnA (particle nanoampere) at inter university accelerator centre (IUAC), New Delhi, India. The low value of current was used to avoid excessive heating of the samples. The cast and dried films were cut into small pieces of size (1×1 cm^2) and were mounted on a vacuum-shielded vertical sliding ladder for irradiation. Irradiation was done at different fluences ranging from 5×10^{10} to 3×10^{12} ion cm^{-2}. The electronic energy loss (S_e) was 59.9 keV μm^{-1} whereas the nuclear energy loss was 0.033 keV μm^{-1} and the range of ion has been calculated by using SRIM-2008 (Stopping and Range of Ions in Matter) and its value was found to be 478 μm for the Li ion. The ions were expected to easily pass through the nanocomposites film samples without implantation because thickness of samples was substantially less than the range of ion beam used for irradiation.

3. Polymer characterization

Each irradiated sample was removed from the irradiation cell before characterization. The changes induced by Li^{3+} ion beam irradiated PLGA nanocomposites were studied using the following techniques:

3.1. X-ray diffraction (XRD)

XRD patterns were recorded on a SHIMADZU 7000-X-ray spectrometer using Cu Kα radiation source. The generator was operated at voltage of 40 KV, current of 30 mA and wavelength used for analysis was 1.54 nm. Samples were placed on a quartz holder and were scanned with 2θ range from 3 to 10° with scan speed of $0.5\ ^\circ\ min^{-1}$.

3.2. Field emission scanning electron microscopy (FESEM)

The surface morphology of pristine and Li ion irradiated PLGA

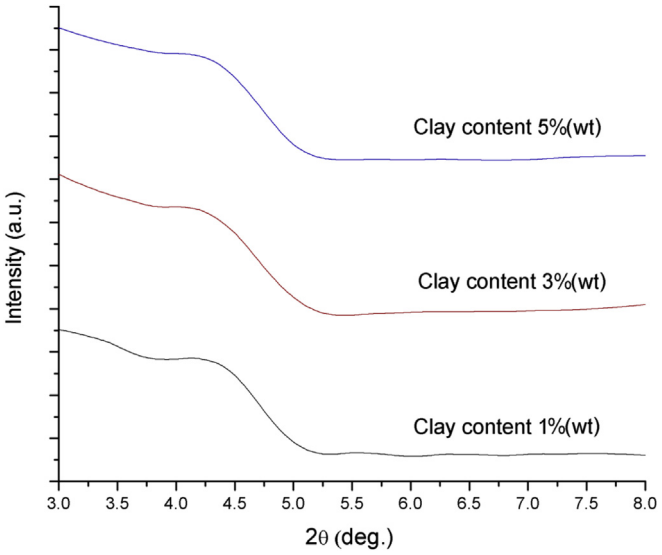

Fig. 1. X-ray diffraction patterns of pristine PLGA/Cloisite® 30B (clay) nanocomposite film samples having 1% (wt), 3% (wt) and 5% (wt) clay content.

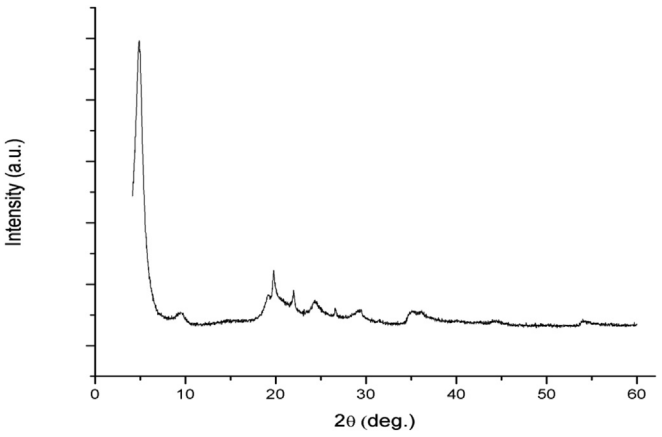

Fig. 2. X-ray diffraction patterns of Cloisite® 30B clay.

nanocomposites were examined using a FESEM (FEI, quanta 200F), which was operated at an accelerating voltage of 5 KV. The film surface was mounted on copper stumps and coated with gold using gold sputter (SCD-005, Sputter coater).

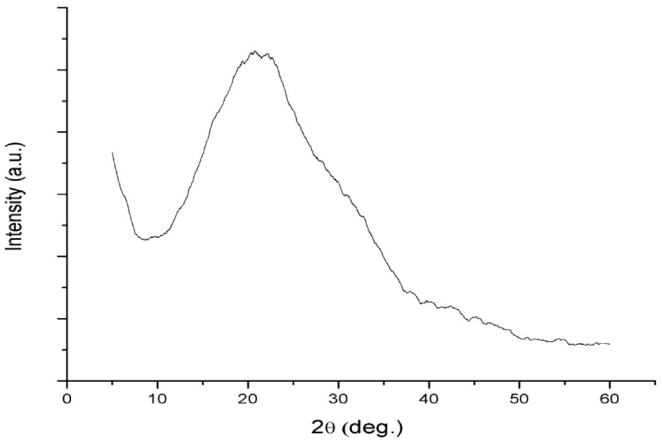

Fig. 3. X-ray diffraction patterns of neat PLGA sample.

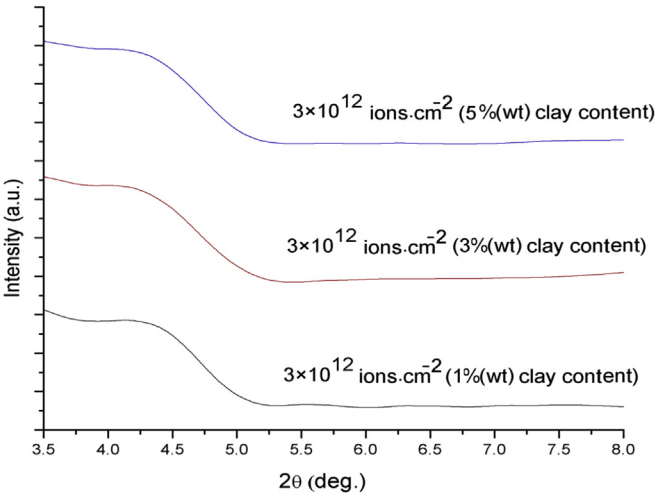

Fig. 4. X-ray diffraction patterns of PLGA/clay nanocomposite of different clay content after irradiation at high fluence of 3×10^{12} ions cm^{-2}.

3.3. Fourier transform infrared (FTIR) spectroscopy

The results of chemical modification of biodegradable polymer nanocomposite can be examined through characterization of vibrational modes determined by FTIR spectroscopy. Cloisite® 30B powder was ground together with dried KBr and compressed at high pressure into a disc. FTIR spectra of this KBr disc, pure PLGA film and its nanocomposite film samples were taken using FTIR-

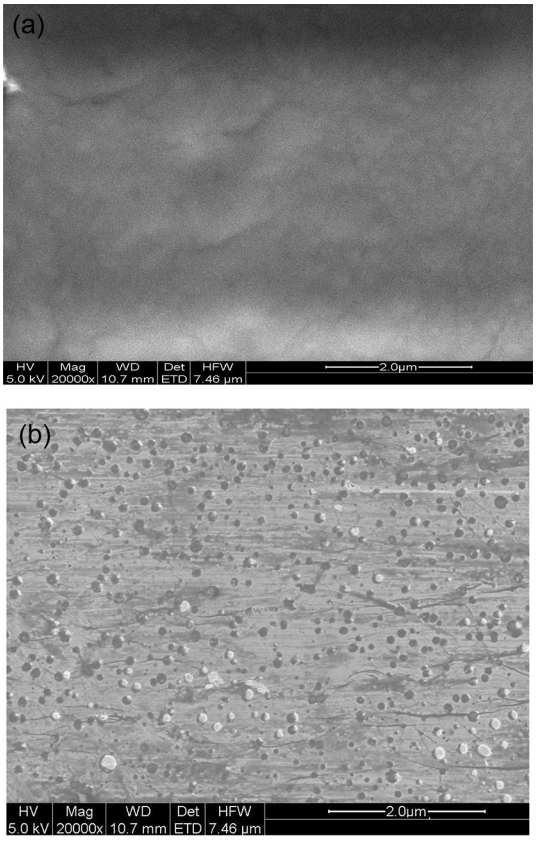

Fig. 5. FESEM images of exfoliated Cloisite 30B-based PLGA nanocomposite, showing (a) fine distribution of the clay in the matrix, and (b) delamination of silicate layers after irradiation.

8400, SHIMADZU in transmission mode with resolution of 2 cm^{-1} in spectral range of 400–4000 cm^{-1}.

3.4. UV–visible spectroscopy

The optical absorption spectra of PLGA nanocomposites were investigated using SHIMAZU UV-1800 spectrophotometer. The wavelength range used for analysis of the spectra was 200–900 nm.

4. Results and discussion

The changes induced in the morphological, optical and structural properties of nanocomposite due to Li^{3+} ion irradiation have been analyzed and the results are discussed here.

4.1. XRD investigation

PLGA/Cloisite® 30B nanocomposite film samples with different loading of nanoclay i.e. 1% (wt), 3% (wt) and 5% (wt) before SHI irradiation have been compared in Fig. 1. In order to detect the d_{001} reflection, effect of SHI irradiation on nanoclay structure and corresponding clay interlayer spacing in various nanocomposites, XRD was performed at low angles ($2\theta < 10^{\circ}$). Typically, a d_{001} peak is observed for 1.8 nm spacing in pure nanoclay (Cloisite® 30B) at $2\theta = 4.9^{\circ}$ as shown in Fig. 2 and a broad amorphous peak of pure PLGA as shown in Fig. 3. If there would have been intercalation between clay layers in the polymer nanocomposites, this peak at $2\theta = 4.9^{\circ}$ would have moved to the left (to lower value of 2θ). From the XRD patterns (for pristine samples (Fig. 1) and for samples irradiated at high fluence of SHI (Fig. 4)), it is difficult to ascertain whether there is intercalation between clay layers or there is complete exfoliation. The diffraction peaks were observed to disappear during irradiation indicating delamination of clay layers resulting in extensive layer separation. SEM images confirmed the X-Ray results as shown in Fig. 5(a, b). However, due to absence of a sharp peak around $2\theta = 4.9^{\circ}$, partial exfoliation can be presumed.

4.2. Effect of SHI on morphology

The gross appearance of amorphous PLGA nanocomposite samples changed from being transparent to yellowish brown upon irradiation at high fluence of SHI beam. The changes occurred in surface morphology of PLGA/clay nanocomposite film samples were examined by FESEM. Figs. 6(a–d), 7(a-c) and 8(a-c) are micrographs of non-irradiated and irradiated nanocomposite samples containing 1% (wt), 3% (wt) and 5% (wt) nanoclay respectively. The appearance of all nanocomposites samples before irradiation seemed to be similar but after being irradiated with SHI at different fluence, they were quite different. The distorted morphology was apparent in all nanocomposite samples after irradiation. The formation of micro holes and cracks in film samples after irradiation by virtue of hydrolytic attack on ester bonds during irradiation. This effect was less pronounced when PLGA nanocomposites were irradiated with low fluence of 5×10^{10} ions cm^{-2} however the defects became more prominent and size of micro holes got enlarged when irradiated with high fluence of SHI beam (3×10^{12} ions cm^{-2}). This clearly indicates chain scission or degradation of PLGA chains and it might release gases like H_2, O_2 and CO_2 etc. as is also reported in a few studies for other degradable polymers [34–36].

From the observed morphology, the clay agglomerations have not been visualized after SHI irradiation, clearly indicating nice dispersion of the clay particles in the polymer matrix. According to Lu et al. [37], free radicals and ions generated with high mobility upon irradiation diffuses in and/or out from the clay galleries. Upon

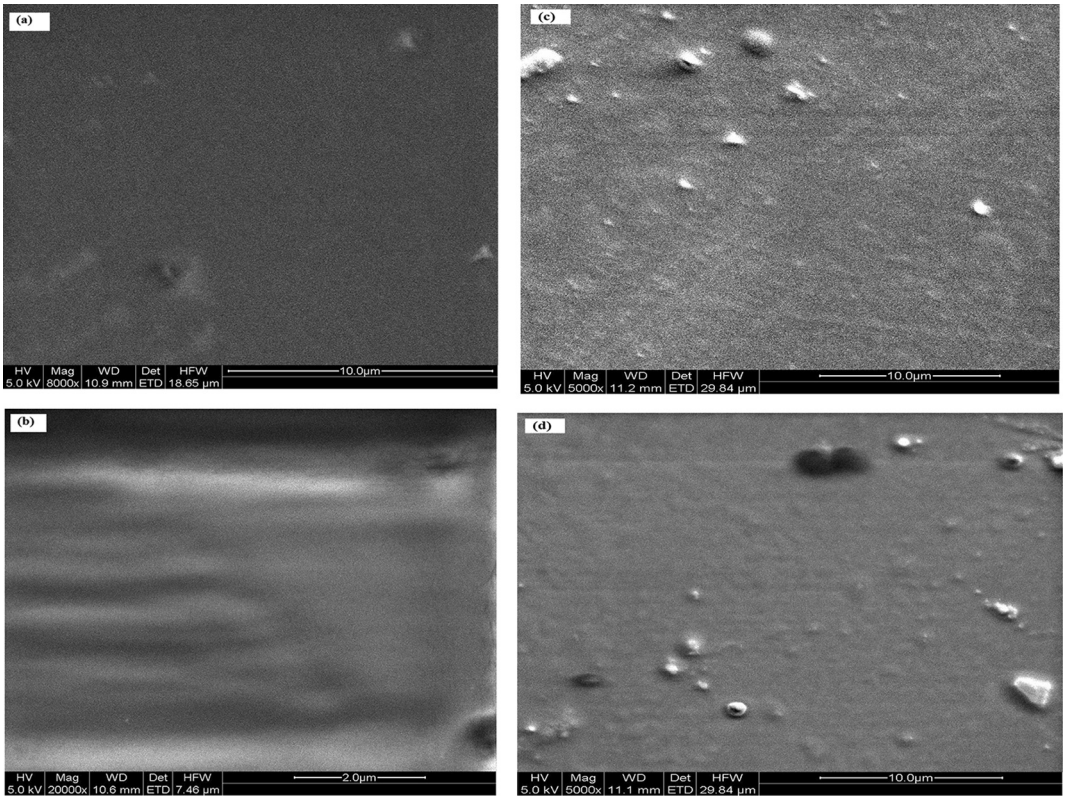

Fig. 6. FESEM images of pristine PLGA and PLGA/clay nanocomposite film samples containing (a) PLGA (b) 1% (wt) clay content (c) 3% (wt) clay content (d) 5% (wt) clay content.

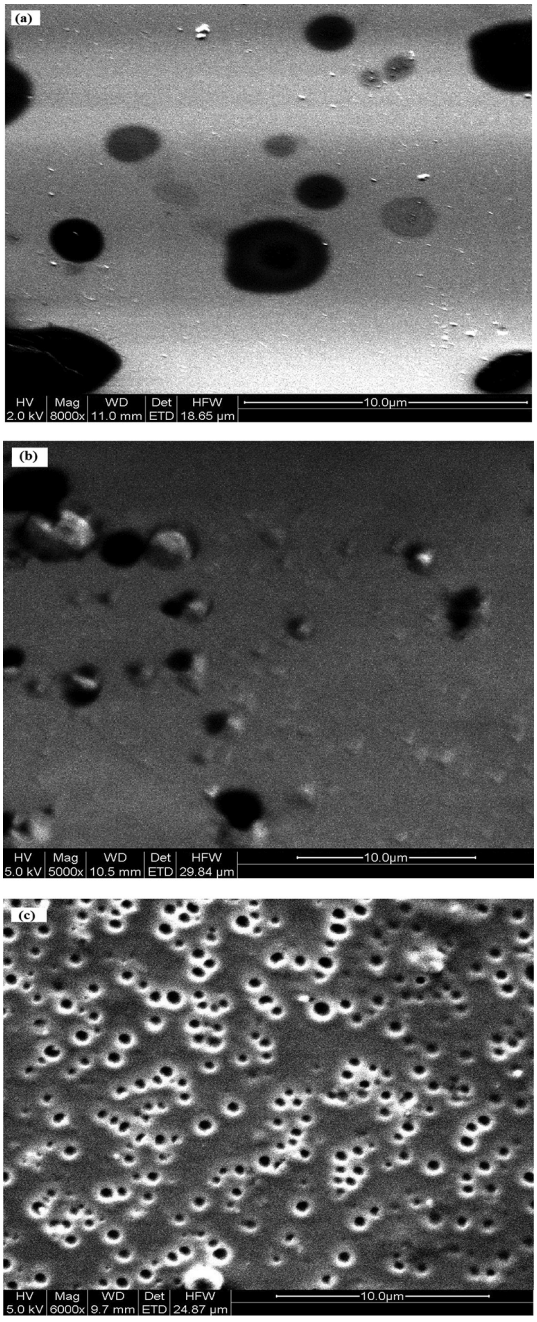

Fig. 7. FESEM images of PLGA/Cloisite® 30B clay nanocomposite film samples (a, b, c) irradiated films by Li^{3+} ion at a fluence of 5×10^{10} ions cm^{-2} for 1% (wt), 3% (wt) and 5% (wt) respectively.

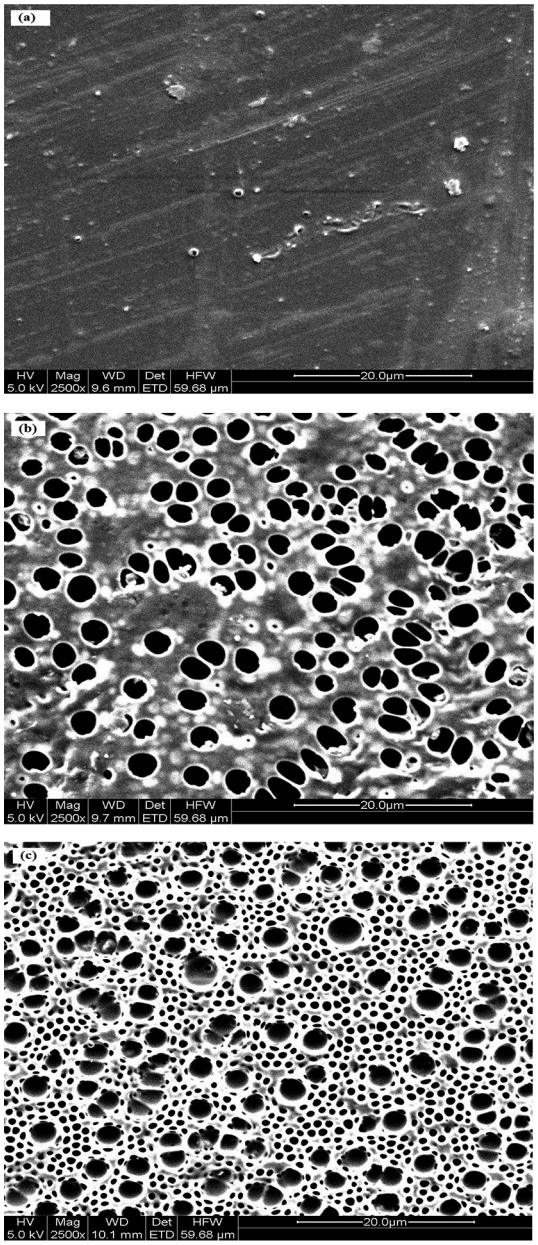

Fig. 8. FESEM images of PLGA/Cloisite® 30B clay nanocomposite film samples (a, b, c) irradiated films by Li^{3+} ion at a fluence of 3×10^{12} ions cm^{-2} for 1% (wt), 3% (wt) and 5% (wt) respectively.

exposure to SHI irradiation, individual silicate layers are free from steric hindrance from adjacent silicate layers. Thus the chains between the clay layers would bond covalently to other chains and the consequent elastic energy would push the clay layers apart to give an exfoliated morphology as shown in Fig. 5(a, b).

Lastly, on re-examining Fig. 8(c, d) (typical SEM images of nanocomposite samples at different loading levels of OMMT i.e. 3% (wt) and 5% (wt) respectively) one interesting observation can be made. The degraded samples can also be looked upon as PLGA/Cloisite® 30B foams. Fig. 8(c, d) shows "holes" throughout the cross-section of material after being irradiated and this micro cellular morphology is similar to a foamed material. Neat nanocomposite do not shows any holes/air pockets which are there in different compositions at different fluences as already shows in Fig. 6(a–c) and 1% (wt) irradiated samples 7(a) and 8(a). At high fluence, the degradation rate of these samples became very large leading to formation of micro cavities. Neat nanocomposite samples or 1% (wt) irradiated samples do not exhibit any micro-cellular structures.

4.3. Analysis of FTIR spectra

FTIR spectra of PLGA/Cloisite® 30B nanocomposite film samples, pristine as well as irradiated with 50 MeV Li^{3+} ions at different fluences are shown in Figs. 9 and 10 respectively.

FTIR of powdered sample of Cloisite® 30B reveals absorption band at 3634 cm^{-1} deriving from O–H stretching for the silicate

group, peak at 1048 cm^{-1} due to Si–O–Si stretching vibration and the organic modifications are responsible for the bands located at 2926 cm^{-1}, 2853 cm^{-1} and 1470 cm^{-1}, which are assigned to C–H vibrations of methylene groups (asymmetric stretching, symmetric stretching and bending respectively) [38,39]. The FTIR peak assignments of pure Cloisite® 30B and of the intercalated clay have been reported by several researchers and agree with the following observations, assignments and interpretations.

The IR spectrum of irradiated nanocomposites is almost similar to that of unirradiated nanocomposite samples. In the irradiated nanocomposite samples, the intensity of absorption peak appearing in the region between 3700 and 3400 cm^{-1} seems to be slightly more at high fluence of Li^{3+} ion which perhaps is due the formation of released H atom from backbone of the polymer with the broken ester linkage after SHI irradiation. During ion beam irradiation these lightest gaseous molecules escape from the polymer causing reduction in H content. When each ion transverse through polymer, it creates the cylindrical zone along ion trajectory and is much effective in releasing H molecules from a polymer, is referred as ion track. However the extent of reduction of H content in polymer during irradiation depends on ion dose, which is the one of accepted mechanism to occur during the irradiation in polymer as also reported in numerous literature [40–42]. But there was not found any appreciable changes in 1800–1600 cm^{-1} region. Upon irradiation, one new small peak with weak intensity was found in nanocomposite samples at around 2340 cm^{-1} which correspond to presence of trapped CO_2 gas upon irradiation with high fluence.

It is observed from the spectra of Cloisite® 30B, the Si–O bending bands (523 cm^{-1} and 465 cm^{-1}) and the relative intensity of very intense Si–O–Si stretching band (1048 cm^{-1}) are most sensitive to the degree of intercalation [43]. These bands are not observed in 1% (wt), 3% (wt) and 5% (wt) irradiated nanocomposite samples, indicating the weak interaction between the clay layers and polymer chain segments supporting the formation of exfoliated morphology. These observations are consistent with Fig. 8 from FESEM that degradation rate increases at high fluence of

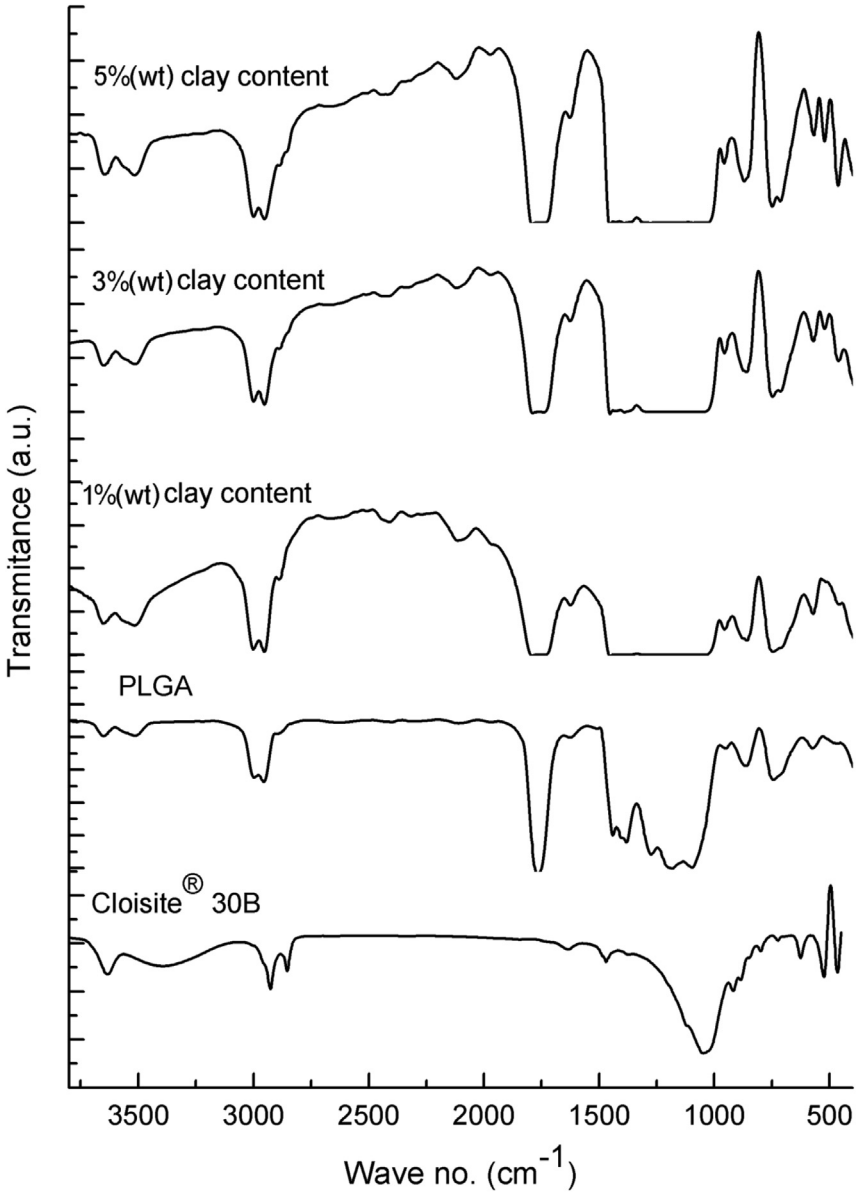

Fig. 9. FTIR spectra of Closite® 30B clay, pure PLGA, and their nanocomposite film samples containing 1% (wt), 3% (wt) and 5% (wt) clay content before irradiation.

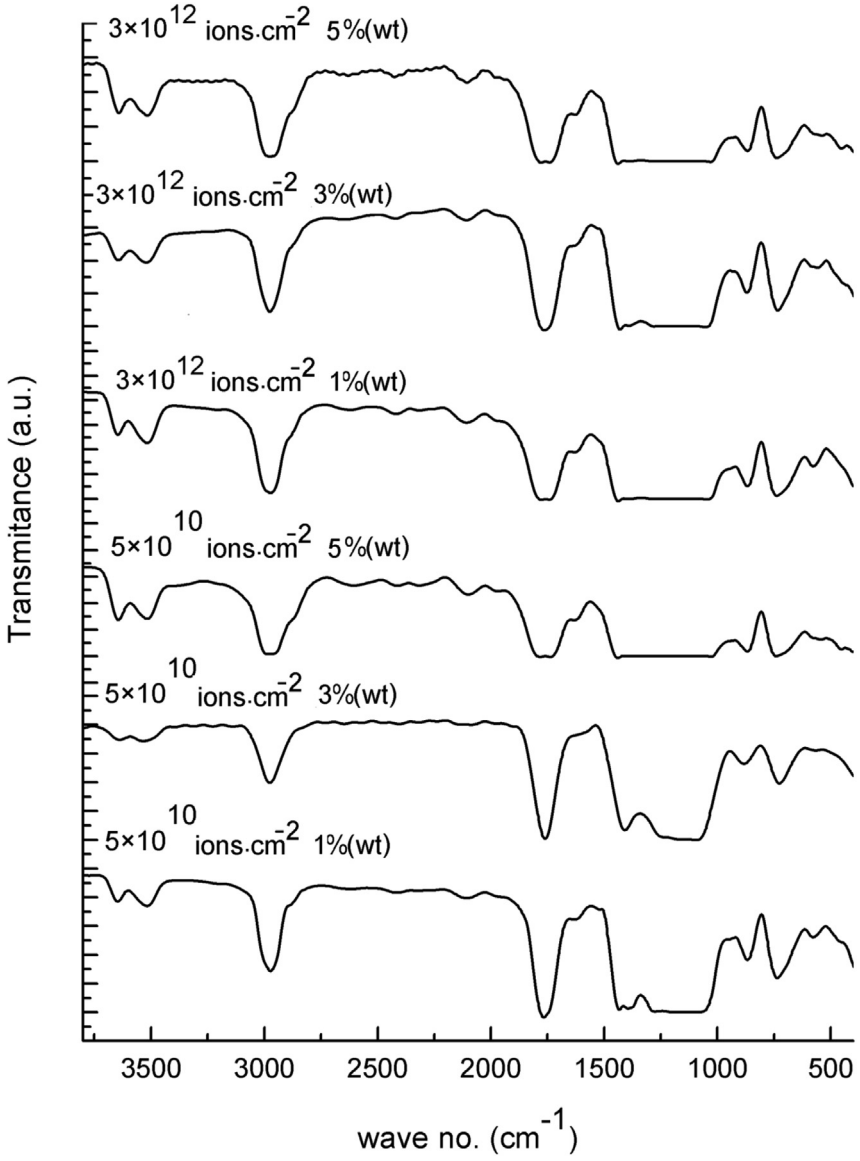

Fig. 10. FTIR spectra of irradiated nanocomposite film samples (containing 1% (wt), 3% (wt) and 5% (wt) clay content) at a fluence of 5×10^{10} ions cm^{-2} and 3×10^{12} ions cm^{-2}.

SHI. The intensity of all peaks in this spectrum reduces with an increase in the ion fluence, which indicates that the crystallinity decreases as a result of SHI irradiation. This result is also supported by XRD spectrum as shown in Figs. 1, 3 and 4 which points the amorphization of irradiated nanocomposite upon SHI irradiation.

4.4. UV–visible spectral analysis

The series of the UV–Visible spectra recorded for Li ion irradiated nanocomposite samples at different fluences are illustrated in Fig. 11. It involves the absorption of UV–visible light by the polymeric material causing the promotion of electrons in σ, π and η orbitals from electronic ground state to a higher excited state and is useful in finding the optical band gap energy (E_g). The optical band gap energy of PLGA nanocomposites have been calculated and are shown in Table 1.

The optical absorption method can be used for the investigation of optically induced transitions and provide information about the energy gap in crystalline and non-crystalline materials [44]. The optical absorption coefficient α(ν) can be correlated to photon energy hν as given by Mott and Davis [45].

$$\alpha(\nu) = B\left[\frac{(h\nu - E_g)^n}{h\nu}\right] \quad (1)$$

where B is constant, hν is the energy of incident photon, E_g (eV) is the optical band gap between the valence band and conduction band and n is the power whose values 1/2, 3/2, 2 and 3 are assumed for direct allowed, direct forbidden, indirect allowed and indirect forbidden transitions respectively. A plot of $(\alpha h\nu)^{1/2}$ versus hν gives the value of E_g. Extending the straight part with abscissa yields the band gap of pristine and irradiated samples. The diffusion of π-electron to the forbidden energy level of polymer causes the irregularities in the band gap level of the polymer. The energy correspond to such diffusion is known as Urbach energy which is calculated from following formula [46].

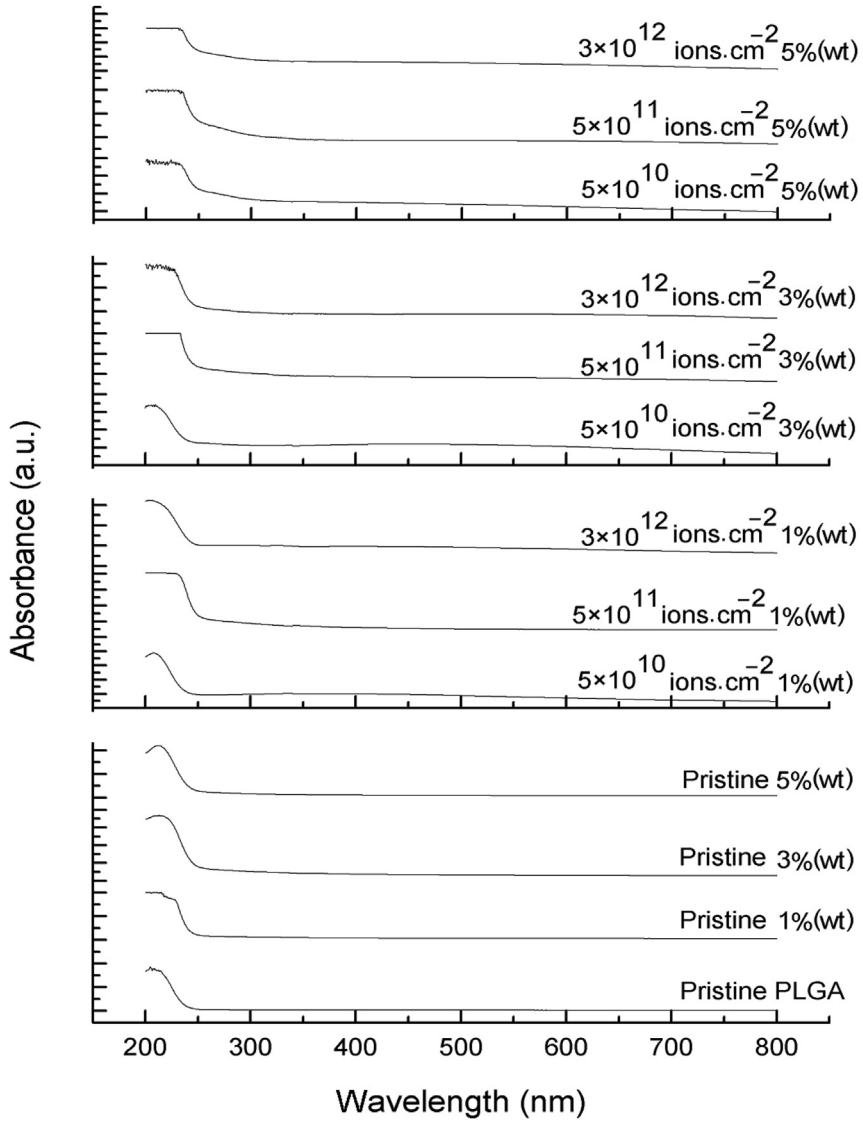

Fig. 11. UV–visible spectra of pristine and Li^{3+} ion irradiated PLGA nanocomposite samples with 1% (wt), 3% (wt) and 5% (wt) clay.

$$\alpha(\nu) = \alpha_0 \exp\left(\frac{h\nu}{E_u}\right) \quad (2)$$

where α_0 is constant, E_u (eV) measure the width tailing of localized states in forbidden gap known as Urbach energy.

The value of Urbach energy increases in 1% (wt) and 3% (wt) nanocomposite samples but at 5% (wt), E_u decreases with increasing fluence which owing to recovery of irregularities in the polymer with cross-linking at high content of clay loading which conceivably slightly increase the band gap in 5% (wt) at high fluence. The optical absorption spectrum of unirradiated PLGA/Cloisite® 30B nanocomposite samples with different clay loading such as 1% (wt), 3% (wt) and 5% (wt), showed a sharp decrease in absorption edge with increasing wavelength up to 251 nm for 1% (wt), 257 nm for 3% (wt), 261 nm for 5% (wt) and 252 nm for neat PLGA followed by a plateau region as shown in Fig. 10. It is evident from Table 1, that after irradiation with Li^{3+} ion at different fluences such as 5×10^{10}, 5×10^{11} and 3×10^{12} ions cm^{-2}, the optical absorption increases with increasing fluence and thus shifts the absorption edge toward the longer wavelength such as visible region for irradiated samples. The increase in optical absorption or change

Table 1
Band gap energy (E_g) and Urbach energy (E_u) in pristine and 50 MeV Li^{3+} ion irradiated PLGA/Cloisite® 30B clay nanocomposite at varying fluences.

Fluence (ions cm^{-2})	1% (wt)		3% (wt)		5% (wt)	
	Bandgap energy (eV)	Urbach energy (eV)	Bandgap energy (eV)	Urbach energy (eV)	Bandgap energy (eV)	Urbach energy (eV)
0	4.88 ± 0.032	0.20	4.70 ± 0.030	0.35	4.68 ± 0.028	0.30
5×10^{10}	4.69 ± 0.023	0.48	4.65 ± 0.013	0.70	4.28 ± 0.018	0.83
5×10^{11}	4.68 ± 0.017	0.40	4.62 ± 0.021	0.58	4.26 ± 0.020	0.69
3×10^{12}	4.58 ± 0.018	0.33	4.50 ± 0.024	0.72	4.30 ± 0.021	0.58

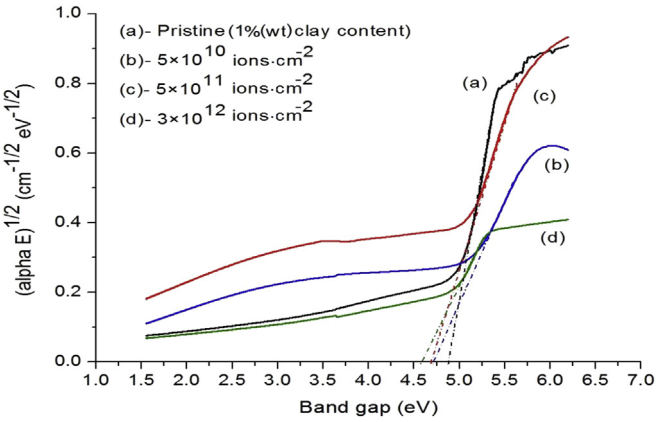

Fig. 12. Extrapolation of Tuac's plot of the pristine and Li^{3+} ion irradiated PLGA nanocomposite samples containing 1% (wt) clay content.

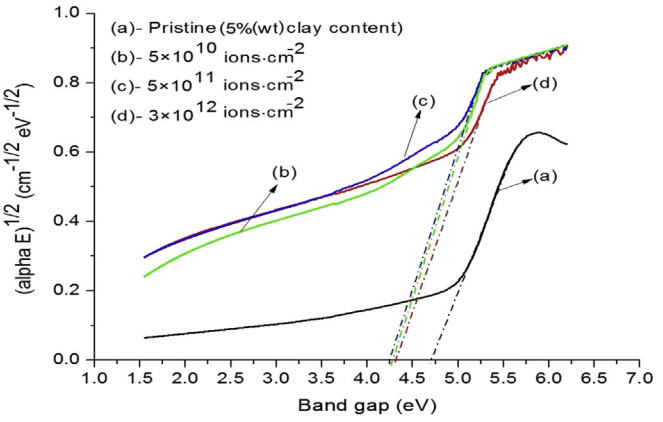

Fig. 14. Extrapolation of Tuac's plot of the pristine and Li^{3+} ion irradiated PLGA nanocomposite samples containing 5% (wt) clay content.

in absorption edge as evident from Fig. 10 possibly attributed to formation of conjugate bonds having wavelength associated to π-π^* transitions and also reflects the decrease in the optical band gap after irradiation. This shift in the absorption edge may be associated to the ion-induced damage and the creation of defects which further results in structural deformation [47–49]. Color changes in the irradiated nanocomposite samples have also been observed at high fluence; possibly ascribed to trapped free radicals or charge species in the polymer matrix. Irradiation induced defects such as anions, cation and free radicals which absorb light during exposure. Due to absorption of radiation, the color of polymer changes from yellow to radish brown and eventually dark brown with higher radiation dose [50–53].

It is observed from Table 1, after irradiated with Li^{3+} ion, the band gap decreases when clay content increases within polymer, which attributed to reduced crosslinking of polymer chains.

Since the glass transition temperature of PLGA matrix is quite low (40–60 °C) and is expected to be easily reached during SHI radiation. Infact, it is quite likely that the ion beam can even locally melt the polymer. So, after irradiation, the nano particles of Cloisite® 30B are easily dispersed within polymer matrix and get cross-linked. The rigid clay platelets which would be thoroughly surrounded by cross linked chains are expected to restrict segmental mobility of molecules and reduce their activity and, consequently decrease the optical band gap as shown in Figs. 12–14. This observation agrees with corroboration by FESEM and FTIR.

The irregularity in the band gap of the film samples are measured in terms of Urbach energy (E_u) and is determined from the inverse of the slope of the plots ln(α) vs. hν. Urbach energy, which is interpreted as the width of the localized states, is used to characterize the degree of disorder in amorphous materials. There is increase in Urbach's energy corresponds to the decrease in optical band gap. The Urbach's energy (E_u) of Li^{3+} ion irradiated nanocomposites has been calculated and is reported in Table 1. The value of Urbach's energy Li^{3+} ion irradiated samples increases at low fluences in 1% (wt) and 3% (wt) nanocomposites samples but in 5% (wt) it decreases at high fluence due to recovery of irregularities in the band gap of polymer with cross-linking at high content of clay loading.

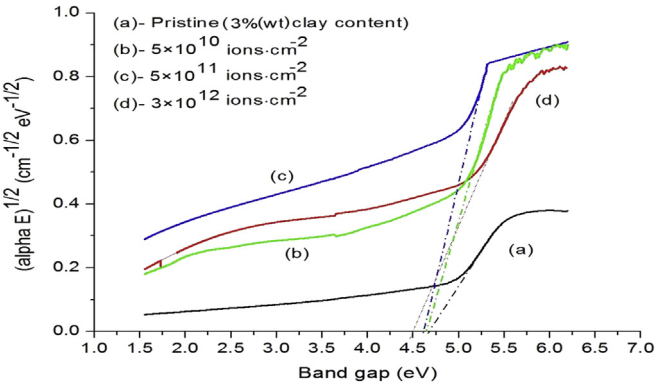

Fig. 13. Extrapolation of Tuac's plot of the pristine and Li^{3+} ion irradiated PLGA nanocomposite samples containing 3% (wt) clay content.

5. Conclusion

Polymer nanocomposites of PLGA have been prepared through the solvent casting route. Irradiation with 50 MeV Li^{3+} ions at fluence range of 10^{10}-10^{12} ions cm^{-2} causes modifications in surface, optical and structural characteristics. XRD measurements show partial exfoliation of clay in PLGA. This was also confirming by FTIR spectra where there was an absence of Si–O–Si stretching (1048 cm^{-1}) and Si–O bending peaks (523 and 465 cm^{-1}) of Cloisite® 30B in nanocomposite. FTIR spectra also exhibited a decrease in the peak intensity after irradiation which suggests the increase in amorphization of nanocomposite after irradiation. UV–visible measurements indicated that the band gap (E_g) values of the nanocomposite samples irradiated with SHI are lower than those of unirradiated samples probably due to sterically interactions between clay layers and reduced cross-linking of polymer chains. This is also supported by FESEM. The morphology evolution of irradiated nanocomposites is also representing the better nano dispersion and steric interactions of clay layers. The service life of nanocomposites has been adversely affected when subjected to ionizing radiation. The brittle nature of PLGA/Clay nanocomposites after radiation is not entirely unexpected since clay is a ceramic. FESEM micrographs of nanocomposites also showed many defects like micro holes and voids when exposed to radiation with increasing ion fluence. This is the first report on the degradable foam formation of PLGA nanocomposites after swift heavy ion irradiation.

Acknowledgment

The authors wish to express gratitude to the authorities of Inter University Accelerator Center (IUAC), New Delhi, India for providing financial assistance in the form of fellowship, beam time and other

facilities. The authors are thankful to Dr. Ramesh Chandra, Institute Instrumentation Center, IIT Roorkee for providing FESEM facilities.

References

[1] M. Okamoto, Polymer/layered Silicate Nanocomposites, Rapra Review Report No. 163, Rapra Technology, London, 2003.
[2] P. Maiti, K. Yamada, M. Okamoto, K. Ueda, K. Okamoto, New polylactide/layered silicate nanocomposites: role of organoclays, Chem. Mater. 14 (2002) 4654–4661.
[3] M.H. Al-Saleh, U. Sundararaj, Processing-microstructure-property relationship in conductive polymer nanocomposites, Polymer 51 (2010) 2740–2747.
[4] N. Groosiord, J. Loos, L. Laake, M. Maugey, C. Zakri, C.E. Koning, A.J. Hart, High-conductivity polymer nanocomposites obtained by tailoring the characteristics of carbon nanotube fillers, Adv. Func. Mater. 18 (2008) 3226–3234.
[5] R. Zhang, Q.Q. Ni, T. Natsuki, M. Iwamoto, Mechanical properties of composites filled with SMA particles and short fibers, Comp. Struc. 79 (2007) 90–96.
[6] P. Meneghetti, S. Qutubuddin, Synthesis, thermal properties and applications of polymer-clay nanocomposites, Thermochim. Acta 442 (2006) 74–77.
[7] D.M. Delozier, R.A. Orwoll, J.F. Cahoon, N.J. Johnston, J.G. Smith, J.W. Connel, Preparation and characterization of polyimide/organoclay nanocomposites, Polymer 43 (2002) 803–812.
[8] D.W. Kim, A. Blumstein, S.K. Tripathy, Nanocomposite films derived from exfoliated functional aluminosilicate through electrostatic layer-by-layer assembly, Chem. Mater. 13 (2001) 1916–1922.
[9] M. Alexander, P. Dubois, Polymer-layered silicate nanocomposites: preparation, properties and uses of a new class of materials, Mater. Sci. Eng. Res. 28 (2000) 1–63.
[10] E.P. Giannelis, Polymer-layered silicate nanocomposites: synthesis, properties and applications, Organomet. Chem. 12 (1998) 675–680.
[11] K. Yano, A. Usuki, A. Okada, T. Kurauchi, O. Kamigaito, Synthesis and properties of polyimide–clay hybrid, J. Poly Sci. A Poly Chem. 31 (1993) 2493–2498.
[12] S.S. Ray, M. Okamoto, Polymer/layered silicate nanocomposites: a review from preparation to processing, Prog. Poly Sci. 28 (2003) 1539–1641.
[13] P. Singh, R. Kumar, UV–visible and infrared spectroscopic studies of Li^{3+} and C^{5+} irradiated PADC polymer, Vacuum 96 (2013) 46–51.
[14] M. Saito, S. Nagata, F. Nishiyama, T. Isshiki, K. Takahiro, Reducing structural change in aluminum coated polyethylene naphthalate foils during MeV proton irradiation, Vacuum 89 (2013) 153–156.
[15] P. Singh, S. Kumar, R. Prasad, R. Kumar, Study of physical and chemical modifications induced by 50 MeV Li^{3+} ion beam in polymers, Radiat. Phys. Chem. 94 (2014) 54–57.
[16] K. Hareesh, P. Sen, R. Bhat, R. Bhargavi, G.G. Nair, Sanjeev G. Sangappa, Proton and alpha particle induced changes in thermal and mechanical properties of Lexan polycarbonate, Vacuum 91 (2013) 1–6.
[17] J.W. Park, J.S. Lee, B. Lee, M. Kim, B.S. Moon, C.Y. Lee, B.H. Choi, Modifications of optical properties of PC/ABS by dual ions beam irradiation, Radiat. Phys. Chem. 84 (2013) 126–128.
[18] R.K. Dhillon, P. Singh, S.K. Gupta, S. Singh, R. Kumar, Study of high energy (MeV) N^{6+} ion and gamma radiation induced modifications in low density polyethylene (LDPE) polymer, Nucl. Instrum. Methods Phys. Res. Sect. B 301 (2013) 12–16.
[19] B.S. Rathore, M.S. Gaur, K.S. Singh, Thermal properties of ion beam irradiated polycarbonate films, Vacuum 86 (2011) 306–310.
[20] V.K. Tiwari, N.K. Singh, D.K. Avasthi, M. Misra, P. Maiti, Swift heavy ions induced controlled biodegradation of poly(ε-caprolactone) nanohybrids, Rad. Phy. Chem. 82 (2013) 92–99.
[21] A. Biswas, R. Gupta, N. Kumar, D.K. Avasthi, J.P. Singh, S. Lotha, D. Fink, S.N. Paul, S.K. Bose, Recrystallization in polyvinylidene fluoride upon low fluence swift heavy ion impact, Appl. Phys. Lett. 78 (2001) 4136–4138.
[22] R. Percolla, L. Calcagno, G. Foti, G. Ciavola, Ordering induced by swift ions in semicrystalline polyvinylidene fluoride, Appl. Phys. Lett. 65 (1994) 2966–2968.
[23] E.H. Lee, Ion-beam modification of polymeric materials: fundamental principles and applications, Nucl. Instrum. Meth. Phys. Res. Sec. B 151 (1999) 29–41.
[24] T. Ichikawa, Mechanism of radiation-induced degradation of poly(methyl methacrylate)—temperature effect, Nucl. Instrum. Meth. Phys. Res. Sec B 105 (1995) 150–153.
[25] S. Shahabi, F. Najafi, A. Majdabadi, T. Hooshmand, M.H. Nazarpak, B. Karimi, S.M. Fatemi, Effect of gamma irradiation on structural and biological properties of a PLGA-PEG-hydroxyapatite composite, Sci. World J. (2014) 1–9. Article ID 420616.
[26] G. Abuhanoğlu, A.Y. Özer, Radiation sterilization of new drug delivery systems, Interv. Med. Appl. Sci. 6 (2014) 51–60.
[27] S. Malathi, P. Nandhakumar, V. Pandiyan, T.J. Webster, S. Balasubramanian, Novel PLGA-based nanoparticles for the oral delivery of insulin, Int. J. Nano Med. 10 (2015) 2207–2218.
[28] N. Arya, D.S. Katti, Poly(d,l-lactide-co-glycolide)–chitosan composite particles for the treatment of lung cancer, Int. J. Nano Med. 10 (2015) 2997–3011.
[29] X. Liu, A.L. Miller, M.J. Yaszemski, L. Lu, Biodegradable and crosslinkable PPF–PLGA–PEG self-assembled nanoparticles dual-decorated with folic acid ligands and Rhodamine B fluorescent probes for targeted cancer imaging, RSC Adv. 5 (2015) 33275–33282.
[30] M. Kaur, S. Singh, R. Mehta, The Effect of O^{6+} and Si^{7+} ion beam irradiations on poly(lactide-co-glycolide) (50: 50) copolymer, Poly Sci. Ser. B 56 (2014) 657–663.
[31] M. Mondragon, J.E. Mancilla, F.J. Rodriguez-Gonzalez, Nanocomposites from plasticized high-amylopectin, normal and high-amylose maize starches, Polym. Eng. Sci. 48 (2008) 1261–1267.
[32] K. Dean, L. Yu, D.Y. Wu, Preparation and characterization of melt-extruded thermoplastic starch/clay nanocomposites, Compos Sci. Technol. 67 (2006) 413–421.
[33] J.R.G. Evans, H.C. Greenwell, P. Boulet, P.V. Coveney, A.A. Bowdenf, A. Whitingc, A critical appraisal of polymer–clay nanocomposites, Chen B. Chem. Soc. Rev. 37 (2008) 568–594.
[34] N. Khalfaoui, C.C. Rotaru, S. Bourard, M. Toulemonde, J.P. Stoquert, F. Haas, C. Trautmann, J. Jensen, A. Dunlop, Characterization of swift heavy ion tracks in CaF_2 by scanning force and transmission electron microscopy, Nucl. Instrum. Meth. Phys. Res. Sec. B 240 (2005) 819–828.
[35] G. Marletta, S. Pignataro, C. Olieri, Correlation between the modification of the chemical structure and the electrical properties of Ar-ion bombarded polyimide, Nucl. Instrum. Meth. Phys. Res. Sec. B 39 (1989) 792–795.
[36] A. Charpiro, Chemical modifications in irradiated polymers, Nucl. Instrum. Meth. Phys. Res. Sec. B 32 (1988) 111–114.
[37] H. Lu, Y. Hu, J. Xiao, Q. Kong, Z. Chen, W. Fan, The influence of irradiation on morphology evolution and flammability properties of maleated polyethylene/clay nanocomposite, Mater. Lett. 59 (2005) 648–651.
[38] P.A. Tarantili, Composites of engineering plastics with layered silicate nanofillers: preparation and study of microstructure and thermo mechanical properties, in: Dr John Cuppoletti (Ed.), Nanocomposites and Polymers with Analytical Methods, 2011, pp. 149–180. USA.
[39] N. Vasanthan, D.R. Salem, Infrared spectroscopic characterization of oriented polyamide 66: Band assignment and crystallinity measurement, J. Polym. Sci. 38 (2000) 516–524.
[40] R.J. Woods, A.K. Pikaev, Applied Radiation Chemistry: Radiation Processing, John Wiley & Sons, Inc., New York, 1994.
[41] A.M. Abdul-Kader, A. Turos, J. Jagielski, L. Nowicki, R. Ratajczak, A. Stonert, M.A. Al-Ma'adeed, Hydrogen release in UHMWPE upon He-ion bombardment, Vacuum 78 (2005) 281–284.
[42] R.L. Clough, High energy radiation and polymers: a review of commercial processes and emerging applications, Nucl. Instrum. Meth. Phys. Res. Sec B 185 (2001) 8–33.
[43] S. Mohamadi, N.S. Sanjani, Studies on PEBAX/organoclay nanocomposites by melt intercalation process: effect of organoclay surface, e-Polymers 135 (2009) 1618–7229.
[44] R. Mishra, S.P. Tripathy, D. Sinha, K.K. Dwivedi, S. Ghosh, D.T. Khathing, M. Muller, D. Fink, W.H. Chung, Optical and electrical properties of some electron and proton irradiated polymers, Nucl. Instrum. Meth. Phys. Res. Sec. B 168 (2000) 59–64.
[45] N.F. Mott, E.A. Davis, Electronic Processes in Non-crystalline Materials, Clarendon, Oxford, 1979.
[46] F. Urbach, The long-wavelength edge of photographic sensitivity and of the electronic absorption of solids, Phys. Rev. 92 (1953) 1324.
[47] N. Betz, M.A. Le, E. Balanzat, J.M. Ramillion, J. Lamotte, P. Gallas, G.J. Jaskierowicz, A FTIR study of PVDF irradiated by means of swift heavy ions, Polym. Ed. B 32 (1994) 1493–1502.
[48] L. Calcagno, G. Compagnin, G. Foti, Structural modification of polymer films by ion irradiation, Nucl. Instrum. Meth. Phys. Res. Sec. B 65 (1992) 413–422.
[49] A.M. Cruzman, J.D. Carlson, J.E. Bares, P.P. Pronko, Chemical and physical changes induced in polyvinylidene fluoride by irradiation with high energy ions, Nucl. Instrum. Meth. Phys. Res. Sec. B 7–8 (1985) 468–472.
[50] R.L. Clough, S.W. Shalaby, Irradiation of Polymers: Fundamentals and Technological Applications, American Chemical Society, Washington, 1996, p. 620.
[51] R.L. Clough, K.T. Gillen, G.M. Malone, J.S. Wallace, Color formation in irradiated polymers, Radiat. Phys. Chem. 48 (1996) 583–594.
[52] R.L. Clough, K.T. Gillen, G.M. Malone, J.S. Wallace, M.B. Sinclair, Discoloration and subsequent recovery of optical polymers exposed to ionizing radiation, Polym. Deg Stab. 49 (1995) 305–313.
[53] K.T. Gillen, J.S. Wallace, R.L. Clough, Dose-rate dependence of the radiation-induced discoloration of polystyrene, Radiat. Phys. Chem. 41 (1993) 101–113.